PHOTOEMISSION INSTABILITIES: THEORY AND EXPERIMENT

Joseph T. Rogers, Laboratory of Nuclear Studies, Cornell University, Ithaca, NY 14853, USA

Abstract

Synchrotron radiation in electron-positron colliders and synchrotron light sources ejects photoelectrons from the beam chamber walls. The resulting cloud of slow photoelectrons interacts with the beam, and may generate a transverse coupled bunch instability. In some high current storage rings a photoemission effect causes the dominant transverse instability, with a sub-millisecond risetime. Two types of photoemission instabilities have been observed. In CESR, photoelectrons are trapped by the combination of a quadrupole electrostatic field from the distributed ion pumps and the field of the bending magnets. This ``trapped photoelectron instability" has a very long range, is nonlinear in beam current, and is predominantly horizontal. In the Photon Factory and BEPC, photoelectrons moving freely across the chamber interact with the positron beam to produce a transverse instability. This ``free photoelectron instability" occurs for bunch-to-bunch intervals smaller than the transit time (a few tens of nanoseconds) of photoelectrons across the chamber, occurs in the absence of external fields, is approximately linear in bunch current, and is predominantly vertical. Numerical simulations of both effects reproduce the observed behavior of the beam, as does an analytical calculation of the trapped photoelectron instability. Experiments to observe these instabilities in other storage rings are underway. There is both theoretical and observational evidence that other types of instabilities due to photoemission may be important. We will discuss the consequences of the photoemission instabilities for the design and operation of high current storage rings.

1 ELECTRON EMISSION PROCESSES

The two main sources of electrons in the beam chamber of a high energy electron or positron storage ring are photoemission and secondary emission. Ionization of the residual gas is negligible source of electrons in comparison to these.

1.1 Photoemission

Electrons are ejected from the beam chamber walls by synchrotron radiation photons. The quantum efficiency of the photoemission process depends on the reflection coefficient of the chamber surface, the angle of incidence of the photons, the photon energy, and the material and surface conditions of the chamber. The reflection coefficient can become large at the shallow angle of incidence typical of synchrotron radiation intercepting beam chamber surfaces. The quantum efficiency tends to increase at low photon energy, and for small angles of incidence, because of the greater probability that an electron liberated close to the surface will penetrate to the surface. Measurements [1] and scaling laws [2] of the photoemission yield have been published, but the dependence on angle of incidence is not fully consistent between different measurements.

As an example, the values of parameters relevant for photoemission in CESR are listed in Table I.

Table I: Photoemission parameters for CESR

parameter	value
beam energy	5.3 GeV
bending radius	88 m
photon critical energy	3.7 keV
$I_{pe}/(I_{beam}/dl)$ (normal incidence)	0.04 m^{-1}
angle of incidence (approx.)	30 mrad
$I_{pe}/(I_{beam}/dl)$ (30 mrad)	0.04 - 0.2 m^{-1}
$I_{pe}/(I_{beam}/dl)$ (from obs. instability)	0.06 m^{-1}

The photoemission rate $I_{pe}/(I_{beam}/dl)$ is calculated by integration over the photon spectrum [1,3], assuming an Al_2O_3 surface on the aluminum vacuum chamber. The uncertainty in the photoemission rate at 30 mrad incidence is due to the uncertainty in the dependence of yield on incidence angle. The photoemission rate in the last row of Table I is inferred from a comparison of the observed photoelectron instability growth rate in CESR and the results of a computer simulation. This is a very large photoelectric current!

1.2 Secondary emission

Secondary electrons may be produced by primary electrons which are accelerated by the close passage of a positron bunch. The secondary electron yield (SEY) depends on the primary electron energy and the material. Aluminum chambers with an Al_2O_3 surface layer have an SEY which reaches a maximum of approximately 2.5 at a primary electron energy of approximately 390 eV [4,5]. All other accelerator vacuum chamber materials have a much lower maximum SEY (typically 1.0 to 1.2).

2 TRAPPED PHOTOELECTRON INSTABILITY

2.1 Observations in CESR

An anomalous transverse coupled bunch instability has been observed for many years in CESR [6,7,8]. The absolute value of the growth rate is largest at the intermediate currents encountered during injection, and becomes dramatically smaller at higher currents. The growth rate of the positron beam is very reproducible and is independent of the residual gas pressure. The instability is not as reproducible for electrons. The instability is predominantly horizontal. Coupled bunch modes at positive frequencies are damped; those at negative frequencies tend to grow. The absolute value of the growth rate decreases monotonically with mode frequency.

0-7803-4376-X/98/$10.00 © 1998 IEEE

If the beam consists of trains of bunches spaced by 28 ns or less, the bunches within a train move coherently.

The anomalous instability is present only when the distributed ion pumps (DIPs) are powered [8]. It disappears immediately when the DIPs are turned off. The growth rate is proportional to the number of DIPs powered and to the DIP anode voltage [9].

CESR contains DIPs in all bending magnets. A series of slots allows gas to flow from the beam chamber to the pump chamber. The slots also allow the DC electric field produced by the DIP anode to leak into the beam chamber, as demonstrated by numerical computation of the potential [10,3].

Some CESR DIPs have copper shields with offset slots, which shield the beam chamber from the DIP field. These shielded pumps have no effect on the beam.

The observations are consistent with the hypothesis [11] that slow electrons trapped in the beam chamber are responsible for the anomalous instability. These electrons are produced primarily through photoemission and are *trapped* in the combined dipole magnetic field and quadrupole electrostatic leakage field from the distributed ion pumps. Repeated passages of the beam eject these photoelectrons. In this way the transverse position of the beam modulates the trapped charge density, which in turn produces a time-dependent force on the beam.

Photoelectrons in the CESR chamber are confined to very small orbits in the horizontal plane by the 0.2 T field of the dipole magnets. The quadrupole component of the leakage field from the DIP slots confines the electrons vertically, much like a Penning trap. Because of the horizontal dipole component of the pump leakage field, the trapped electrons undergo an $\mathbf{E}\times\mathbf{B}$ drift down the length of the magnet, with a velocity of the order of 10^3 m/s, and are lost from the magnets in a few milliseconds. Electrons are removed by interactions with the beam on a time scale of tens of microseconds [3], so electron loss by drift is negligible. The cyclotron frequency of the trapped electrons is 5.6 GHz, so their cyclotron motion is unimportant at the frequencies of the coupled bunch modes. The vertical motion of the electrons, with frequencies of several MHz, dominates the dynamics.

2.2 Computer simulation

A computer simulation of photoelectron trapping was produced to calculate the coupled bunch growth rate and tune shift in CESR [3]. In this model, the trajectories of electron macroparticles moving under the influence of the electric field of the distributed ion pumps, a bunched beam, and the space charge of the other photoelectrons are calculated. Only vertical motion of the electrons is allowed because of the strong dipole magnetic field.
Macroparticle velocities and positions and the electric field are updated each time step of 0.5 ns. If the trajectory of the macroparticle has taken it outside the chamber boundaries, it is removed. Secondary emission is modeled by injecting one or more macroparticles, depending on the secondary emission efficiency, which is a function of the incident macroparticle energy. During the beam passage, smaller time steps are used in which several photoelectron macroparticles are injected with a uniform distribution of velocities. A value of the photoemission efficiency for the aluminum chamber which nearly reproduces the measured current dependence of the instability growth rate. This value is consistent with the extrapolation of the photoemission rate measured at DCI [1] to CESR parameters shown in Table I.

Figure1 shows the calculated electron charge density 10 ns after the passage of a leading bunch in the present CESR pattern of 9 trains of 2 bunches, with bunches in a train separated by 28 ns. The pumping slots are to the left, and the beam is at the origin. Newly emitted photoelectrons are evident as bands at the top and bottom of the chamber. Photolectrons which have been slowed by the space charge of the leading photoelectrons may be trapped on low-amplitude trajectories. The passage of subsequent bunches eventually ejects these trapped electrons.

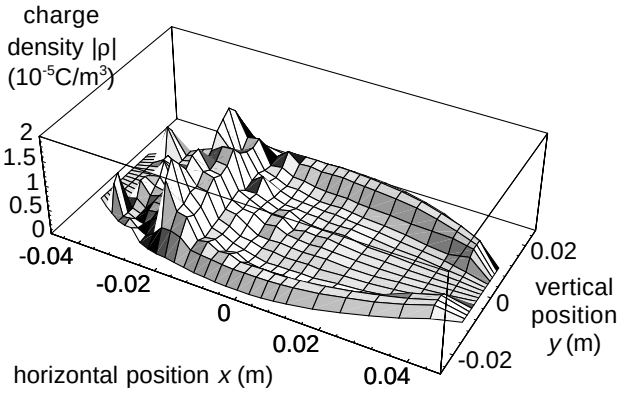

FIG. 1 Calculated charge density in the CESR beam chamber 10 ns after the passage of a bunch.

The growth rate of the lowest frequency coupled bunch mode was calculated from the force on the horizontally oscillating beam. The growth rate for the 9×2 bunch pattern is shown in Fig.2. The error bars on the simulation points show the effect of the limited number of macroparticles. The simulation shows chaotic behavior which leads to a large scatter in the calculated growth rates

. 2.3 Analytical model

An approximate analytical model of photoelectron trapping which predicts the scaling of the growth rate with frequency and with current has been produced [12]. The time-varying force on the beam occurs because the strength of the repeated small kicks which remove the trapped electrons depends on the beam position. Because the electrons move in the nonlinear potential produced by the DIP and space charge, these kicks occur at nearly random phases of the trapped electron oscillation, and the motion of the electrons resembles diffusion. We model the diffusive motion of the electrons using a continuous Fokker-Planck equation.

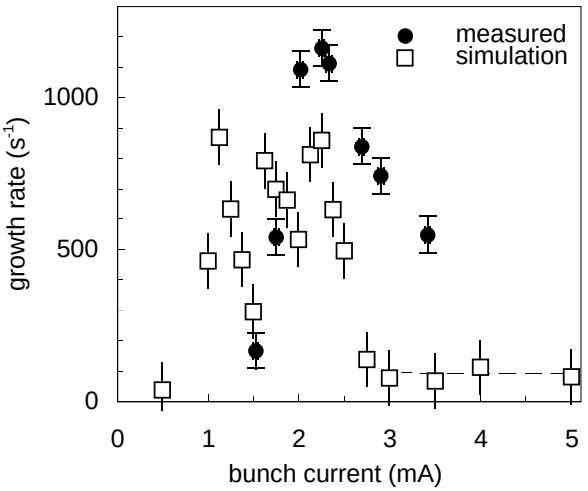

FIG. 2. Horizontal betatron growth rates in s^{-1} vs. bunch current in mA for the lowest frequency mode, measured in CESR and calculated by the simulation program. The curves are meant only to guide the eye.

We reduce the problem to a single spatial dimension by assuming that there is no variation of the forces or the diffusion constant in the region of trapped electrons, because the electrons are confined to a small band within the region between the beam and the DIP slots, as demonstrated by the numerical simulation, and further simplify the problem using the fact that the vertical oscillation period of the trapped electrons is much shorter than the characteristic time for electrons to diffuse out to the chamber wall. The phase space distribution will be approximately symmetric with respect to the phase of the oscillation.

The calculated growth rate is shown in Fig. 3 for the lowest frequency horizontal mode. These growth rate curves, plotted as a function of bunch charge, agree well with observations in CESR [7,9] The same model constants are used to fit three bunch data from 1985 and 9×2 bunch data from 1995.

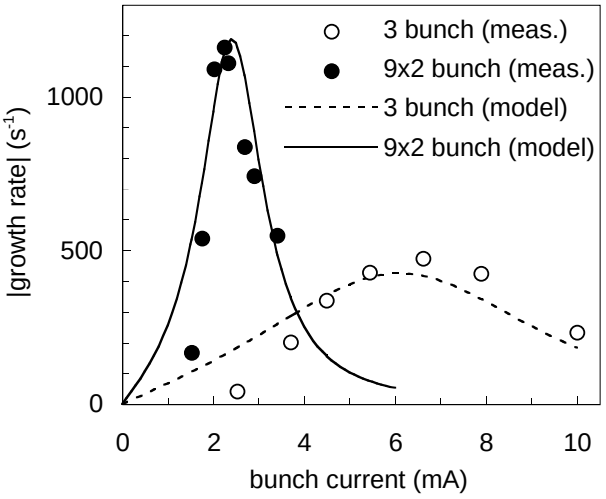

FIG. 3. Horizontal betatron growth rates in s^{-1} vs. bunch current in mA for the lowest frequency mode, measured in CESR (points) and calculated by the photoelectron model (curves).

3 ELECTRON CLOUD (FREE PHOTOELECTRON) INSTABILITY

In contrast with the trapped photoelectron instability observed in CESR, strong evidence for a *free* photoelectron instability (electron cloud instability or "ECI") has been observed in the Photon Factory and BEPC. This instability, in contrast with the CESR instability, occurs in the absence of magnetic and electrostatic fields; occurs only for positron beams, because electron beams repel the photoelectrons; is strong in the vertical direction; and increases with beam current. It is short-range in nature, because the photoelectrons move rapidly to the chamber walls. This free photoelectron instability is not observed in CESR, which operates with widely spaced bunches.

3.1 Observations in Photon Factory

A vertical coupled bunch instability has been observed with positron beams in the Photon Factory [13]. This instability has a very low threshold current (15 - 20 mA), shows a spectrum of betatron sidebands that is broad in frequency, and persists when a gap is introduced into the bunch pattern. The instability is observed with as few as 37 successive bunches followed by 275 empty buckets. The bands of excited betatron sidebands move to lower frequency as the beam current increases, indicating that the instability is not due to electromagnetic modes in beam chamber structures.

When an electron beam is used in the PF, a vertical instability with a higher current threshold and a completely different spectrum is observed. This latter instability is consistent with ion trapping, and is suppressed by a gap in the bunch pattern

The instability in the PF is consistent with an interaction of the positron beam with free photoelectrons. The electron beam is unaffected because the photelectron are repelled by the beam. A computer simulation of the electron cloud instability [14] (described below) reproduces the behavior of the observed instability.

3.2 Observations in BEPC

An instability similar to the one seen in the PF has been observed at BEPC by an IHEP/KEK collaboration in an extensive set of measurements [15]. As in the PF, the instability is vertical, appears only with positron beams, shows a broad distribution of betatron sidebands, and persists with a large gap in the bunch pattern. It has a low current threshold, similar to that in the PF.

The dependence of the instability threshold and beam spectrum on a large number of parameters was investigated. It was found that these did depend on the vertical chromaticity, the bunch spacing, the beam energy, the horizontal beam emittance, and the RF frequency (which moves the horizontal closed orbit).

The current threshold was observed to increase from 10 mA to 40 mA with only alternate RF buckets filled. This is consistent with the evidence from computer simulations, which show that the average electron density increases with decreasing bunch spacing [3,16]. The dependence of the instability threshold on energy is

weaker than that expected for an instability generated by electromagnetic wake fields. Further analysis of the large body of data is continuing, and more measurements are planned.

3.3 Computer simulations

Computer simulations of the electron cloud instability have been used to reproduce the observed effects [14] and to design beam chambers for new storage rings [16]. These simulations track electron macroparticles under the influence of the fields of the beam and electron space charge, and include photoemission and secondary emission models. The effective "wake" due to the electron cloud is determined by displacing a single bunch from the design orbit and calculating the force on subsequent bunches. This wake potential may then be Fourier transformed to determine the effective impedance.

4 LESSONS FROM THE SIMULATIONS

4.1 Role of bunch pattern

The transit time of the electrons across the beam chamber sets a time scale for the electron cloud instability. The electrons pass across the chamber in approximately 10 to 100 ns. The free photoelectron instability only occurs when the bunch spacing is smaller than this time interval. In contrast, the trapped photoelectron instability seen in CESR is seen even with a single bunch in the storage ring, because the electrons are trapped for many turns of the beam.

In the electron cloud instability, the cloud is established in approximately 100 ns, and disappears after a similar time in the absence of beam. The instability is thus expected to be insensitive to a gap in the bunch pattern, as is observed in the PF and BEPC.

For very closely spaced bunches, the presence of a trapping potential is unimportant, as the chamber will contain a high electron density with or without such a potential. Fig. 4a shows the calculated electron charge density in the CESR chamber in the presence of the DIP leakage field, as a function of bunch spacing and charge, and Fig. 4b shows the calculated charge density in the absence of the DIP leakage field

4.2 Bunch length

In the dipole magnets, cyclotron motion of the electrons may be excited by successive bunch passages [16]. Large horizontal momenta are possible after repeated beam passages. This effect is suppressed if the bunch passes in a time that is longer than one cyclotron period. This bunch length condition is satisfied for existing and planned storage rings.

4.3 Secondary emission

If the secondary emission yield is sufficiently high, an avalanche of secondary electrons can occur [16]. The electron density then increases until it is limited by its own space charge. This density is much higher that the density in the absence of runaway secondary emission, and may produce a much higher instability growth rate. With a lower SEY, the contribution of secondary electrons to the electron density may still be important.

In the regime where electron trapping is important (*i.e.*, long bunch spacing), secondary emission has a negligible effect [3,12].

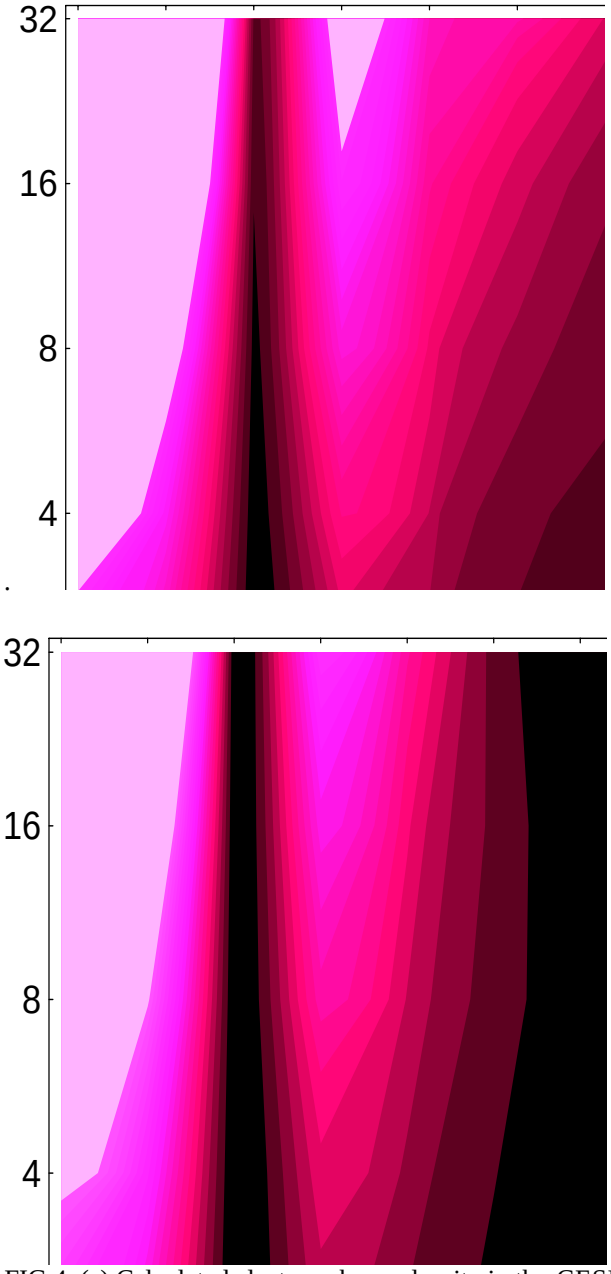

FIG 4. (a) Calculated electron charge density in the CESR chamber in the presence of the DIP leakage field, as a function of bunch spacing (ns) and bunch charge (10^{10} e). Contours are 1 nC/m, with black representing zero. (b) Calculated charge density in the absence of the DIP field.

4.4 Space charge

In the trapped electron instability, the electron "lifetime" is of the order of 10μs. The trapped electron density increases until limited by its own space charge. Space charge is always important in this instability [3,11,12].

In contrast, the electron lifetime in the electron cloud instability is of the order of 100 ns. In the absence of a secondary emission runaway condition, space charge is relatively unimportant [16].

5 CONTROL OF THE INSTABILITIES

The photoelectron instabilities may be controlled by

- Eliminating any trapping potential. In newly designed storage rings the DIPs have been isolated from the beam chamber by lengthening the pumping slots. In CESR, the DIP voltage has been reduced from 7.3 kV to 1.9 kV. The photoelectron trapping instability growth rate is found to be proportional to the DIP voltage [9].
- Using an antechamber to absorb sychrotron radiation far from the beam.
- Suppressing secondary emission with low SEY materials (such as Cu or stainless steel) or coatings (such as TiN, used in PEP-II).
- Increasing the bunch spacing. This may be impractical due to other design constraints, but is a very effective way to suppress the electron cloud instability.
- Damping the instability with beam feedback. This has been done in CESR and is planned for all of the new high current storage rings.

6 CONCLUSIONS

The photoelectron instabilities may be the dominant transverse instabilities in high current electron and positron storage rings. The calculated and measured growth rates, of the order of 1 ms^{-1}, are high and close to the maximum that may be controlled with present beam feedback systems. Good observations have been made in CESR, the Photon Factory, and BEPC, but observations in other machines, particularly ones with different chamber geometries, would be very useful. The basic mechanisms are understood, but more work is necessary to gain a detailed understanding. Computer simulations have successfully reproduced the features of the instability, but these are time consuming, and a means of simply estimating the threshold and growth rate of the electron cloud instability is lacking at present. The growth rate is fast, but the instabilities can be controlled with a combination of chamber geometry, materials, and beam feedback.

7 ACKNOWLEDGMENTS

The author wishes to thank and acknowledge the contributions of T. Holmquist, K. Ohmi, M. Furman, Z.Y. Guo, S. Heifets, J. Byrd, M. Billing, D. Sagan, D. Hartill, D. Rice, E. Chojnacki, and Y. Li as well as the other members of the CESR Operations Group.
The work at CESR has been supported by the National Science Foundation.

REFERENCES

[1] Gröbner, et al., J. Vac. Sci. Technol. **A7**, 223 (1989).
[2] Kobayashi, Proc. 5th Symp. Accelerator Sci. & Technol., 250 (1984).
[3] Holmquist, M.S. thesis, Cornell Univ. (1996).
[4] Landolt-Börnstein II/6, Springer-Verlag (1959).
[5] von Ardenne, Tabellen der electronenphysik, ionenphysik und übermikroskopie, Deutscher Verlag de Wissenschaften (1956).
[6] Sakazaki, R.M. Littauer, R.H. Siemann, and R.M. Talman, IEEE Trans. Nucl. Sci. 32, 2353 (1985).
[7] Sakazaki, Ph.D. thesis, Cornell Univ. (1985).
[8] Littauer, Cornell LNS report CLNS 88/847 (1988).
[9] Hartill, T. Holmquist, J.T. Rogers, and D.C. Sagan, Cornell LNS report CBN 95-3 (1995).
[10] Sagan and J.J. Welch, Cornell LNS report CBN 92-1 (1992).
[11] Rogers, Proc. 1995 Particle Accelerator Conf., Dallas, 3052 (1995).
[12] Holmquist and J.T. Rogers, "The trapped photoelectron instability in electron and positron storage rings", submitted to Phys. Rev. Lett. (1997).
[13] Izawa, Y. Sato, and T. Toyomasu, Phys. Rev. Lett. **74**, 5044 (1995).
[14] Ohmi, Phys. Rev. Lett. **75**, 1526 (1995).
[15] Guo, et al., "The Experimental Study on Beam-Photoelectron Instability in BEPC", this conference.
[16] Furman and G.R. Lambertson, Proc. 1996 European Particle Accelerator Conf., Barcelona, 1087 (1996), and "The Electron-Cloud Instability in PEP-II", this conference.